

## Research Article

# Measurement and Analysis of Local Average Power According to Averaging Length Changes of 3, 6, 10, and 17 GHz in an Indoor Corridor Environment

Seong-Hun Lee <sup>1</sup> and Byung-Lok Cho <sup>2</sup>

<sup>1</sup>Industry-Academic Cooperation Foundation, Suncheon National University, Jungang-ro 255, Suncheon-si, Jeollanam-do 57922, Republic of Korea

<sup>2</sup>Division of Electrical and Electronics Engineering, Suncheon National University, Jungang-ro 255, Suncheon-si, Jeollanam-do 57922, Republic of Korea

Correspondence should be addressed to Byung-Lok Cho; [blcho@suncheon.ac.kr](mailto:blcho@suncheon.ac.kr)

Received 15 September 2022; Revised 18 November 2022; Accepted 11 January 2023; Published 20 January 2023

Academic Editor: Shobhit K. Patel

Copyright © 2023 Seong-Hun Lee and Byung-Lok Cho. This is an open access article distributed under the Creative Commons Attribution License, which permits unrestricted use, distribution, and reproduction in any medium, provided the original work is properly cited.

This study measures and analyzes the local average power for line-of-sight (LOS) and non-line-of-sight (NLOS) paths according to the averaging length in an indoor corridor environment. The indoor corridor comprises multiple offices, laboratory spaces, and lecture rooms. We selected 3, 6, 10, and 17 GHz measurement frequency bands. The measurement system consists of a signal generator, a low-noise amplifier, transmission and receiving antenna, and spectrum analyzer. To obtain an accurate prediction model of propagation due to the multipath effect, we determined the measurement method based on the measurement interval and number of measurements according to changes in the averaging length. 2, 4, 6, 8, and 10 lambdas ( $\lambda$ ) were selected for the number of measurements by frequency, and 1.5 cm was set as the measurement interval. We used the close-in (CI) path loss model for the analysis according to changes in the averaging length. The coefficient of determination ( $R$ -squared) was applied using a linear regression equation to verify the measurement accuracy. Based on parameter  $n$  of the CI path loss model, no large differences were observed in the averaging length at each measurement frequency. However, at  $2\lambda$ , owing to the multipath effect,  $R$ -squared was approximately 0.4–0.7 for the LOS path and 0.6–0.8 for the NLOS path. At  $10\lambda$ ,  $R$ -squared was approximately 0.7–0.8 for the LOS path and 0.8–0.9 for the NLOS path. This indicated that as the number of measurements increased by increasing the averaging length, the accuracy of the measurement results improved. The study findings will help determine an optimal averaging length, thus ensuring reliable indoor propagation measurement and contributing to the ITU-R standard.

## 1. Introduction

Recent rapid advancements in wireless communication technologies have made frequency allocation crucial. The frequency bands of interest are microwaves and millimeter waves. Researchers are developing new propagation models for these frequency bands [1, 2]. In a multipath fading or short-term fading environment of mobile radio, researchers discovered that the appropriate length to obtain the local average power is in the  $20\lambda$ – $40\lambda$  wavelength range [3]. In an indoor multipath propagation environment, the local average power-signal strength has been estimated using power

accumulation and the  $10\lambda$  linear average at 900 MHz and 2 GHz frequencies [4]. In addition, by simulating the 2.4 GHz frequency in an indoor multipath propagation environment, researchers estimated the local average power-signal strength based on the size, spacing, and arrangement [5]. Although path loss models have been presented for 8, 9, 10, and 11 GHz in indoor corridors and office environments [6], there is no mention of a local average power measurement method or the coefficient of determination using linear regression analysis. As described in [7], an indoor corridor environment has multiple reflections and waveguide effects. Through recommendation P.1238-10 [8], the

ITU-R is working to standardize indoor environment parameters for developing propagation models [9, 10]. Measurement methods for indoor environments must measure the local average power to account for the multipath effect. Moreover, when measuring local average power, considering the number of measurements according to changes in the averaging length is necessary.

This study measures local average power in an indoor corridor environment with severe multipath conditions. We analyzed the local average power measurements at optimal averaging lengths for 3, 6, 10, and 17 GHz frequencies. The reasons for choosing the frequencies 3, 6, 10, and 17 GHz are as follows: ITU-R P.1238-10 [8] is a contribution on indoor radio-wave data and prediction models with frequencies 300 MHz–450 GHz. Table 2 of ITU-R P.1238-10 contains a list of corridor environments and no propagation model parameter values corresponding to frequencies of 3, 6, 10, and 17 GHz. Therefore, measurement data and propagation-model parameter values corresponding to the frequencies of 3, 6, 10, and 17 GHz are required. In addition, measurement data and propagation model parameter values for the 3, 6, 10, and 17 GHz bands are written and adopted in Report ITU P.2406-2 [11]; these frequencies were used in this study. To verify the local average power measurement results, we applied them to the close-in (CI) path loss model, a propagation prediction model. Furthermore, we obtained the coefficient of determination using a linear regression equation [12, 13] and performed a comparative analysis.

## 2. Materials and Methods

**2.1. Measurement Environment and System.** Section 6.1.7.4 of ITU-R Report P.2406-2 [11] presents the indoor corridor environment, measurement scenario, and measurement system of Building No. 1, College of Engineering, Sunchon National University. This study used identical frequency bands, measurement environment, measurement scenario, and measurement system. Figure 1 displays the measurement environment and scenario. The measurement environment comprised offices, laboratories, and lecture rooms along an indoor corridor. In addition, the measurement scenario and pictures 1–24 are numbered in the figure, and it shows the location and status of the surrounding environment. The types of materials are represented by different colors. We used two measurement locations (Tx) for the measurement scenario. Tx 1 and Tx 2 are the line-of-sight (LOS) and non-line-of-sight (NLOS) path measurements, respectively. We collected measurement data at 0.5 m intervals and measured the local average power at all Rx points. We measured all distances in 3D. The measurement system comprised a signal generator, a signal analyzer, low-noise amplifier, transmission and receiving antenna, and cables. We used a rail with a maximum length of 1 m to measure the local average power.

**2.2. Measurement Method.** Owing to the loss due to multipath propagation in the indoor environment, a local average power method is needed to obtain precise

measurement data. Equation (1) is used for applying the local average power method, and the three parameters are the averaging length ( $L$ ), number of samples ( $N$ ), and interval between samples ( $d$ ) [4, 5].  $N$  varies according to the changes in  $L$  and  $d$ . The value of  $d$  was fixed at 1.5 cm, and the results according to the change in  $L$  were analyzed.  $2\lambda$ ,  $4\lambda$ ,  $6\lambda$ ,  $8\lambda$ , and  $10\lambda$  were applied to change  $L$ . Table 1 lists the number of measurements at each frequency according to the averaging length. Figure 2 shows the diagram of the rail for the local average power measurement system and a photograph of the developed system. The Autonics A15K-S545-G10 motor is manufactured by incorporating the rail so that the Rx antenna can move via motor control. The rail had a maximum length of 1 m, and the Rx antenna moved along the rail with a measurement interval of 1.5 cm.

$$L = Nd. \quad (1)$$

## 3. Results and Discussion

We used the CI path loss model for the analysis according to changes in the averaging length. Equation (2) represents the CI path loss model presented in ITU-R P.1238-10 [8]. To consider shadow effects, we added the last term,  $X_\sigma$ . The parameter  $N$  was  $10n$ . The coefficient of determination ( $R$ -squared) was calculated using a linear regression equation to verify the measurement accuracy. We calculated  $R$ -squared using the linear regression equation provided by the curve fitting toolbox of MATLAB. Figures 3 and 4 present graphs of the CI path loss model at  $2\lambda$ ,  $4\lambda$ ,  $6\lambda$ ,  $8\lambda$ , and  $10\lambda$  of the LOS path and NLOS path, respectively. Table 2 lists the corresponding result values. Table 2 shows the power loss coefficients ( $n$ ), standard deviation ( $\sigma$ ), and  $R$ -squared of the CI path loss model parameters at  $2\lambda$ ,  $4\lambda$ ,  $6\lambda$ ,  $8\lambda$ , and  $10\lambda$  for the LOS and NLOS paths. The values of parameter  $n$  at  $2\lambda$  and  $10\lambda$  for the LOS path are 1.36 and 1.36 at 3 GHz, 1.44 and 1.41 at 6 GHz, 1.41 and 1.39 at 10 GHz, and 1.51 and 1.49 at 17 GHz, respectively. The error is 0–0.02 for each measurement frequency of the LOS path. The values for the NLOS path are 2.46 and 2.42 at 3 GHz, 2.68 and 2.61 at 6 GHz, 2.60 and 2.56 at 10 GHz, and 2.74 and 2.67 at 17 GHz. The error is 0.04 to 0.07 for each measurement frequency of the NLOS path. Based on the error of parameter  $n$  of the CI path loss model, we observed no large differences in the averaging length at each measurement frequency. The  $R$ -squared values at  $2\lambda$  and  $10\lambda$  for the LOS path are 0.66 and 0.83 at 3 GHz, 0.51 and 0.79 at 6 GHz, 0.43 and 0.71 at 10 GHz, and 0.75 and 0.82 at 17 GHz. The values for the NLOS path are 0.80 and 0.95 at 3 GHz, 0.66 and 0.73 at 6 GHz, 0.68 and 0.82 at 10 GHz, and 0.74 and 0.88 at 17 GHz. For the LOS and NLOS paths, the  $R$ -squared values at  $10\lambda$  are higher than at  $2\lambda$ . The  $R$ -squared values at all frequency bands for the LOS and NLOS paths are at least 0.5 and close to 1, indicating high reliability at  $10\lambda$ , which has a higher number of measurements than at  $2\lambda$  or other averaging lengths. The graphs in Figures 3 and 4 show that at  $2\lambda$ , the values measured along the line of best fit of the measurement



FIGURE 1: Scenario of the measured indoor corridor environment [11].

TABLE 1: Measurement points of local average power.

Frequency (GHz)	Measurement points				
	$2\lambda$	$4\lambda$	$6\lambda$	$8\lambda$	$10\lambda$
3	13	27	41	53	67
6	7	13	21	27	33
10	5	9	13	17	21
17	3	5	7	9	11

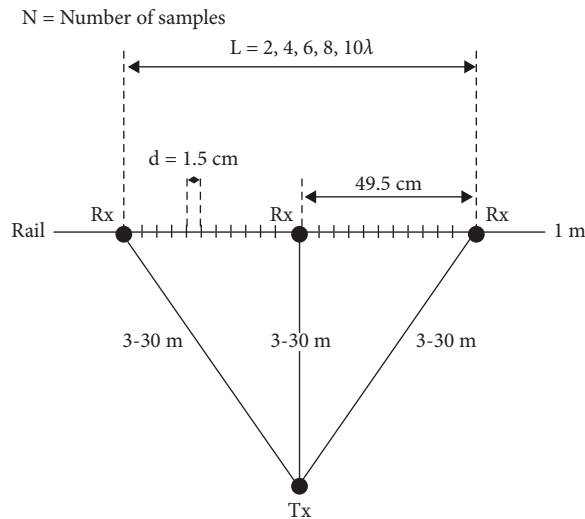


FIGURE 2: Rail of the local average power measurement. (a) Schematic. (b) Prototype.

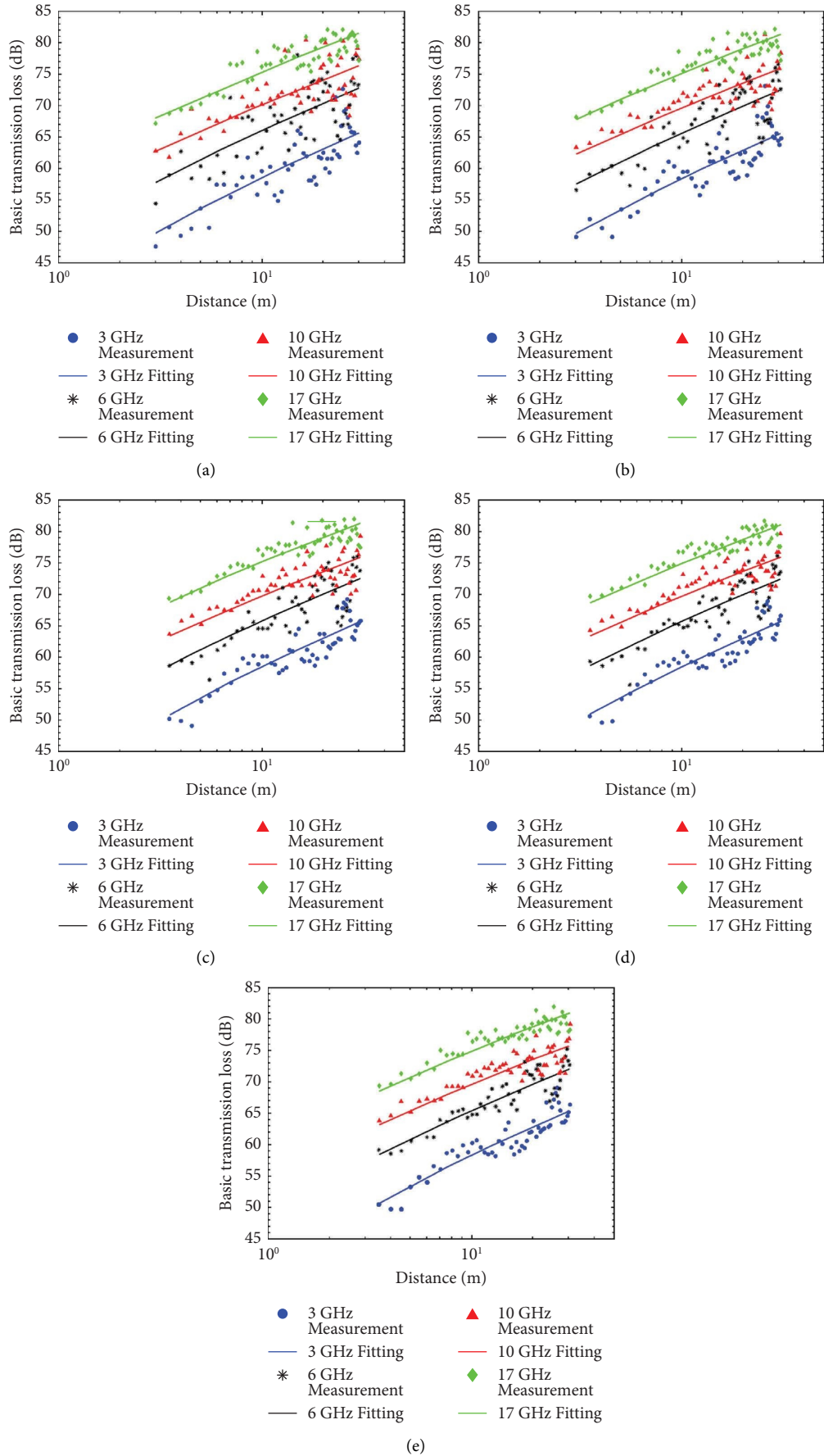


FIGURE 3: Measurement and fitting results of LOS. (a)  $2\lambda$ . (b)  $4\lambda$ . (c)  $6\lambda$ . (d)  $8\lambda$ . (e)  $10\lambda$ .

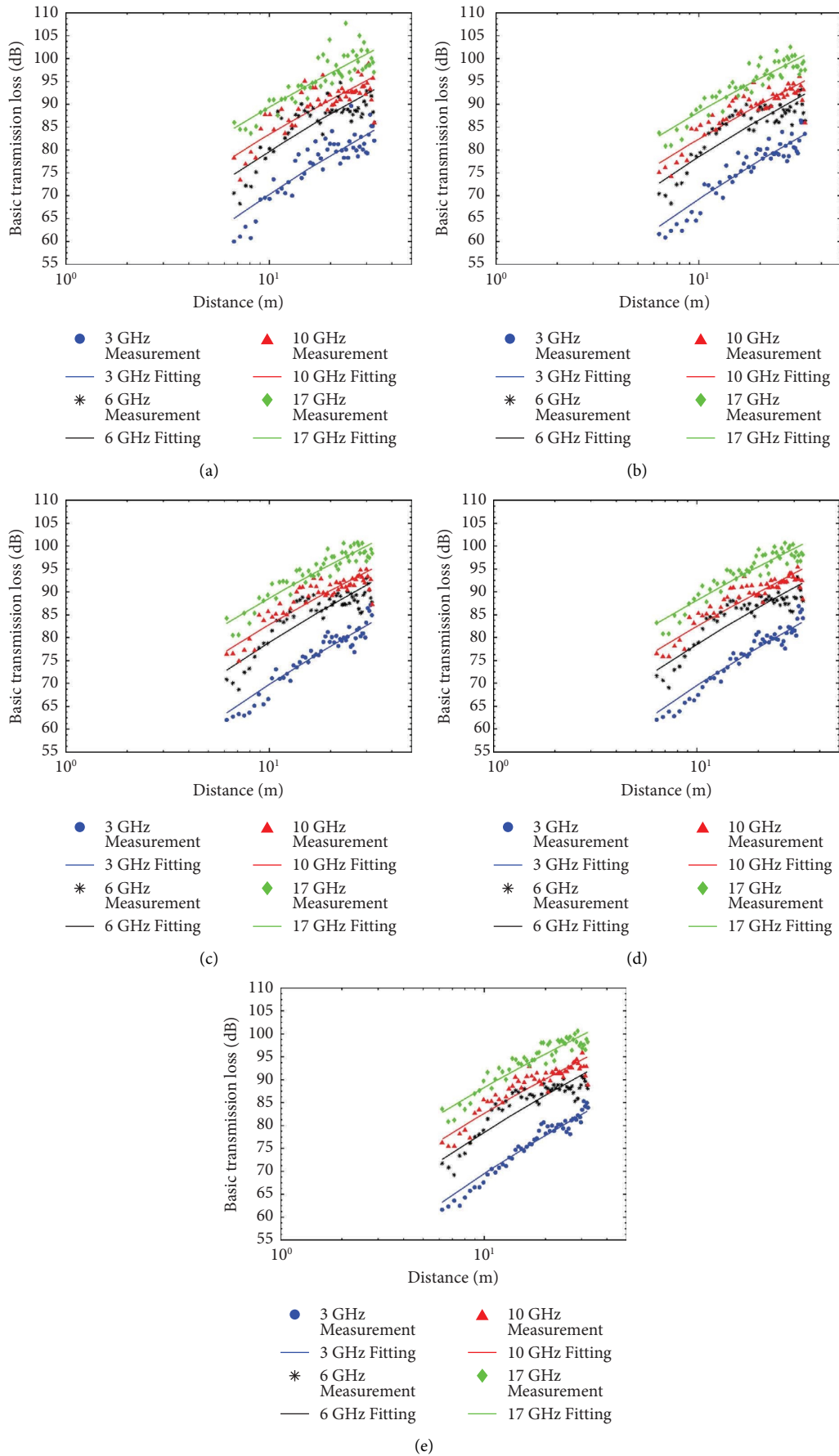


FIGURE 4: Measurement and fitting results of NLOS. (a)  $2\lambda$ . (b)  $4\lambda$ . (c)  $6\lambda$ . (d)  $8\lambda$ . (e)  $10\lambda$ .

TABLE 2: Power loss coefficients, standard deviation, and  $R$ -squared of measured parameters.

Frequency (GHz)	LOS			NLOS		
	$n$	$\sigma$	$R$ -squared	$n$	$\sigma$	$R$ -squared
$2\lambda$						
3	1.36	2.81	0.66	2.46	2.70	0.80
6	1.44	3.69	0.51	2.68	3.54	0.66
10	1.41	3.47	0.43	2.60	3.22	0.68
17	1.51	2.07	0.75	2.74	3.26	0.74
$4\lambda$						
3	1.36	2.48	0.70	2.44	2.03	0.88
6	1.42	3.17	0.60	2.64	2.98	0.71
10	1.38	2.76	0.50	2.57	2.69	0.74
17	1.51	1.95	0.75	2.70	2.36	0.85
$6\lambda$						
3	1.36	1.96	0.79	2.43	1.72	0.91
6	1.43	2.75	0.69	2.62	2.85	0.72
10	1.38	2.30	0.60	2.55	2.47	0.76
17	1.51	1.80	0.78	2.68	2.09	0.87
$8\lambda$						
3	1.36	1.77	0.82	2.43	1.56	0.93
6	1.43	2.47	0.74	2.62	2.73	0.72
10	1.39	2.15	0.64	2.55	2.27	0.80
17	1.49	1.60	0.80	2.67	2.06	0.87
$10\lambda$						
3	1.36	1.63	0.83	2.42	1.25	0.95
6	1.41	2.08	0.79	2.61	2.59	0.73
10	1.39	1.92	0.71	2.56	2.16	0.82
17	1.49	1.52	0.82	2.67	1.94	0.88

frequency are highly dispersed. When  $10\lambda$  is applied, however, the measured values are concentrated along the line of the best fit of the measurement frequency.

$$PL_{CI} (dB) = L(d_0) + N \log_{10} \left( \frac{d}{d_0} \right) + X_{\sigma}, \quad (2)$$

where

$N$ : distance power loss coefficient ( $N = 10n$ )

$d$ : separation distance ( $m$ ) between the base station and portable terminal (where  $d > 1$  m)

$L(d_0)$ : basic transmission loss at  $d_0$  (dB), for a reference distance  $d_0$  at 1 m, assuming free-space propagation  $L(d_0) = 20 \log_{10} f - 28$ , where  $f$  is in MHz

$d_0$ : reference distance ( $m$ )

$X_{\sigma}$ : standard deviation (dB)

#### 4. Conclusions

In a measurement scenario of an indoor corridor environment, this study measured and analyzed local average power according to the transmitter and receiver positions in the 3, 6, 10, and 17 GHz frequency bands for LOS and NLOS paths. We configured the measurement environment, scenario, and system identical to those presented in Section 6.1.7.4 of ITU-R Report P.2406-2 [11]. As a measurement method, we selected  $2\lambda$ ,  $4\lambda$ ,  $6\lambda$ ,  $8\lambda$ , and  $10\lambda$  for the local

average power measurement. The rails of the local average power measurement system were designed and fabricated. As for the measurement results and analysis, the parameter  $N$  value of the CI path loss model did not significantly vary with the averaging length. At  $2\lambda$ , owing to the multipath effect,  $R$ -squared was approximately 0.4–0.7 for the LOS path and 0.6–0.8 for the NLOS path. At  $10\lambda$ ,  $R$ -squared was approximately 0.7–0.8 for the LOS path and 0.8–0.9 for the NLOS path, indicating that the accuracy of the results improved as the number of measurements increased owing to the change in the average length. If an averaging length higher than  $10\lambda$  is selected, the reliability increases as the number of measurements increases. A local average measurement method was used to obtain accurate measurement data according to loss due to multiple paths in the indoor environment. The interval between samples was fixed as 1.5 cm, and the number of measurements due to the change in the average length was determined. Reference data for selecting the averaging length was proposed using the  $R$ -squared value. However, as the number of measurements increases, the measurement time and size of the local average device increase, leading to spatial limitations. Therefore, an appropriate averaging length must be selected for the measurements. In addition, as the number of measurements increases owing to an increase in the averaging length in the measurement results, the correlation owing to the large number of samples at 3 GHz is high, but that owing to the relatively small number of samples at 17 GHz is low. In addition to the appropriate selection of the averaging length,

various directions of analysis should be considered by appropriately using various measurement intervals and the same number of measurements for each measurement frequency.

In the future, we expect the findings of this study to significantly contribute to selecting averaging lengths for measuring local average power in an indoor corridor environment and presenting coefficients of determination for the accurate reliability of prediction models. Furthermore, we expect the data obtained in this study to be used as a reference for the ITU-R standard.

## Data Availability

The data used to support the findings of this study are available from the corresponding author upon request.

## Conflicts of Interest

The authors declare that there are no conflicts of interest regarding the publication of this paper.

## Acknowledgments

This work was supported by the ICT R&D program of MSIP/IITP (2018-0-01439, Analysis of Radio Propagation Characteristics and Development of Prediction Models in Indoor and Outdoor Environments below 40 GHz).

## References

- [1] A. C. M. Austin, D. Guven, M. J. Neve, and K. W. Sowerby, "60 Ghz millimetre-wave channel characterisation for indoor office environments," in *Proceedings of the European Conference on Antennas and Propagation (EuCAP 2019)*, Krakow, Poland, April 2019.
- [2] G. R. Maccartney, T. S. Rappaport, S. Sun, and S. Deng, "Indoor office wideband millimeter-wave propagation measurements and channel models at 28 and 73 GHz for ultradense 5G wireless networks," *IEEE Access*, vol. 3, pp. 2388–2424, 2015.
- [3] W. C. Y. Lee, "Estimate of local average power of a mobile radio signal," *IEEE Transactions on Vehicular Technology*, vol. 34, no. 1, pp. 22–27, 1985.
- [4] R. A. Valenzuela, O. Landron, and D. L. Jacobs, "Estimating local mean signal strength of indoor multipath propagation," *IEEE Transactions on Vehicular Technology*, vol. 46, no. 1, pp. 203–212, 1997.
- [5] H. Obeidat, A. A. S. Alabdullah, N. T. Ali et al., "Local average signal strength estimation for indoor multipath propagation," *IEEE Access*, vol. 7, pp. 75166–75176, 2019.
- [6] I. D. S. Batalha, A. V. R. Lopes, J. P. L. Araújo et al., "Indoor corridor and office propagation measurements and channel models at 8, 9, 10 and 11 GHz," *IEEE Access*, vol. 7, pp. 55005–55021, 2019.
- [7] N. O. Oyiye and T. J. O. Afullo, "Measurements and analysis of large-scale path loss model at 14 and 22 GHz in indoor corridor," *IEEE Access*, vol. 6, pp. 17205–17214, 2018.
- [8] International Telecommunication Union, "Propagation data and prediction methods for the planning of indoor radio-communication systems and radio local area networks in the frequency range 300 MHz to 450 GHz," *Recommendation ITU-R P.1238-10*, pp. 1–27, Springer, Geneva, Switzerland, 2021.
- [9] N. R. Zulkefly, T. A. Rahman, M. H. Azmi, and O. A. Aziz, "6.5 GHz and 10.2 GHz path loss measurements and modeling for 5G communications system prediction," *International Journal of Renewable Energy Technology*, vol. 6, no. 11, pp. 6–11, 2017.
- [10] A. F. Molisch, "Ultra-wide-band propagation channels," *Proceedings of the IEEE*, vol. 97, no. 2, pp. 353–371, 2009.
- [11] ITU Radiocommunication Sector, "Studies of short-path propagation data and models for terrestrial radio-communication systems in the frequency range 6 GHz to 450 GHz," Report ITU-R P.2406-2, pp. 1–151, ITU Radiocommunication Sector, Geneva, Switzerland, 2021.
- [12] S. K. Patel, J. Surve, V. Katkar et al., "Encoding and tuning of THz metasurface-based refractive index sensor with behavior prediction using XGBoost regressor," *IEEE Access*, vol. 10, pp. 24797–24814, 2022.
- [13] S. K. Patel, J. Surve, J. Parmar, A. Natesan, and V. Katkar, "Graphene-based metasurface refractive index biosensor for hemoglobin detection: machine learning assisted optimization," *IEEE Transactions on NanoBioscience*, pp. 1–8, 2022.